

# Novel Ergodic Capacity Upper Bound for Dual-Branch MIMO Ricean Systems

Michail Matthaiou, *Student Member, IEEE*, Yannis Kopsinis, *Member, IEEE*,  
David I. Laurenson, *Member, IEEE*, and Akbar M. Sayeed, *Senior Member, IEEE*

## Abstract

In this paper, a novel analytical upper bound on the ergodic capacity of Multiple-Input Multiple-Output (MIMO) communication systems is derived, based on a key power normalization. Given their high practical usability, we are particularly interested in dual-branch configurations where both the transmitter (Tx) and receiver (Rx) deploy two antenna elements. Contrary to the majority of related studies, where only the common case of Rayleigh fading was considered, our analysis is extended to account for the generalized case of Ricean fading where a deterministic Line-of-Sight (LoS) component exists in the communication link and both ends are affected by spatial correlation. In the following, it is clearly shown that the proposed bound is not only remarkably simple and efficient but also applicable for any arbitrary system Signal-to-Noise Ratio (SNR) and rank of the mean channel matrix. The tightness of the bound is also explored where it is demonstrated that as the SNR tends to zero the bound becomes asymptotically tight; at high SNRs, the offset between empirical capacity and the proposed bound is analytically computed which implies that an explicit asymptotic capacity expression can ultimately be obtained.

## Index Terms

MIMO channels, ergodic capacity, Ricean fading, spatial fading correlation.

M. Matthaiou, Y. Kopsinis and D. I. Laurenson are with the Institute for Digital Communications, Joint Research Institute for Signal and Image Processing, School of Engineering and Electronics, The University of Edinburgh, The King's Buildings, EH9 3JL, Edinburgh, U.K. (e-mail:{M.Matthaiou, Y.Kopsinis, Dave.Laurenson}@ed.ac.uk).

A. M. Sayeed is with the Department of Electrical and Computer Engineering, University of Wisconsin-Madison, Madison, WI 53706, USA (e-mail:akbar@engr.wisc.edu).

## I. INTRODUCTION

Over the last years, a considerable amount of research interest has been devoted to the study of Multiple-Input Multiple-Output (MIMO) systems in response to the increasing demand for higher data rates and improved reliability in wireless communications. The pioneering works of Foschini [2] and Telatar [1] demonstrated the dramatic performance enhancement when multiple antenna elements are employed at both ends of a radio link; in fact, it was theoretically shown that in rich scattering environments the ergodic MIMO capacity can increase linearly with the minimum number of transmit and receive antennas. In order to comprehend in depth the advantages of this promising technology, one of the most interesting topics that needs to be addressed is the derivation of efficient and elegant analytical capacity bounds. By doing so, it is anticipated that the design of practical and simulated MIMO systems as well as the construction of optimized space-time codes would be enriched.

The majority of related studies documented in literature consider the tractable case of Rayleigh fading where no direct Line-of-Sight (LoS) is present in the radio channel and a high multipath activity occurs as a result of the surrounding scattering environment. For this specific case of Rayleigh conditions, a plethora of results is available for various scenarios spanning from uncorrelated fading to double-sided spatial correlation (see for instance [1]–[5] and references therein among others). In most real-time channels though, the assumption of Rayleigh fading is often violated due to either a specular wavefront or a strong direct component. In such a case, the entries of the channel matrix can be more effectively modeled by the Ricean rather than Rayleigh distribution. Surprisingly, despite their high practical relevance, significantly fewer publications focusing on MIMO Ricean channels have been reported. This fact can be attributed to the difficulty in manipulating hypergeometric functions with two matrix arguments of non-central Wishart matrices, as they appear in Ricean channel models, compared to the one matrix argument of central (zero-mean) Wishart matrices tied to Rayleigh fading.

The most important investigations dealing with the ergodic capacity of Ricean-fading MIMO channels can be found in [6]–[20]. More specifically, in [6] the distribution of the ergodic capacity for independent and identically distributed (i.i.d.) rank-1 Ricean-fading channels was explored at the high Signal-to-Noise (SNR) regime. In [7], explicit closed-form expressions for the ergodic capacity were presented via infinite series while in [8] capacity statistics (mean and second-order moment) were expressed in integral form for arbitrary rank of the mean channel matrix. An interesting approach is reported in [9] where upper and lower numerical bounds were derived for the i.i.d. case, assuming that the transmit side has knowledge of statistical properties of the fading process but not of the instantaneous channel state information (CSI).

The first analytical bounds on MIMO Ricean capacity can be found in [10]–[12] where the assumption of uncorrelated fading at both ends was adopted. In [13], [14], these results were extended to account for spatial correlation at a single end of the MIMO link. The more general case of double-sided spatial correlation was addressed in [15], [16], using elements of quadratic form theory. The main characteristic of the above cited papers though ([10]–[16]), is that they are limited to the case of rank-1 LoS matrices. While this condition occurs quite often in reality as a result of the excessive correlation of the LoS' rays phases, at the same time, is not sufficiently general since it limits the applications of MIMO technology to conventional configurations.

To the best of the authors' knowledge, the derivation of capacity bounds in the general case of arbitrary-rank mean matrices, has been separately assessed in [17], [18] and [19]. The former paper proposed a very tight lower bound on the ergodic capacity of semi-correlated MIMO Ricean channels after decomposing the channel correlation matrix into non-central Wishart submatrices and thereafter applying the bounding technique originally proposed in [5]. In [18], the authors relied on the expected values of elementary functions of complex non-central Wishart matrices to come up with an efficient capacity upper bound of semi-correlated MIMO Ricean channels. The latter paper represents so far the more general approach in the associated area since it derives several lower and upper bounds assuming all different types of spatial correlation. However, the paper's general upper bound is given as an infinite summation of Hayakawa polynomials of one matrix argument, which the authors acknowledge as quite involved and computationally inefficient. We also refer to the work presented by Lozano *et al.* [20], who considered the high-SNR capacity offsets in order to establish the key effect of the so-called power offset on MIMO performance. Summarizing, it appears that no tractable analytical results exist in the literature for the upper bound of double-sided correlated MIMO systems in Ricean fading with arbitrary-rank of the deterministic component.

On these grounds, in the present paper, using some recent results on the theory of Wishart matrices and quadratic forms, we derive a novel and efficient upper bound on the ergodic capacity of dual-branch MIMO systems, using the prevalent power constraint in the literature. Hereafter, the term dual-branch or simply dual will stand for MIMO systems where both the transmitter (Tx) and receiver (Rx) are equipped with two antenna elements. We put emphasis on the fact that these configurations are expected to be employed in the majority of future practical systems (e.g. hand-held devices), thanks to their small size and low complexity/implementation cost. Most importantly, several key simplifications are made possible as a result of the compact matrix sizes involved in the mathematical derivations.

In order to formulate a broad framework, we consider the effects of spatial correlation at both ends

and, further, allow the rank of the mean channel matrix to be arbitrary. More specifically, we explore two different class of MIMO systems, namely a conventional low-rank (LR) and a specifically-designed high-rank (HR) configuration, which benefits from the presence of LoS components and yields the highest possible capacity for a given Ricean  $K$ -factor [21]–[23]. The tightness of the bound is also investigated in detail and it is clearly shown that as the SNR tends to zero the bound becomes asymptotically tight while the offset from true capacity is analytically determined as well, for infinitely high SNRs.

The remainder of the paper is organized as follows: In Section II, some basic definitions related to non-central Wishart matrices and quadratic forms are outlined, since they are essential in order to comprehend the following theoretical analysis. In Section III, the underlying MIMO Ricean channel model used throughout the paper is discussed along with the statistics of the channel matrix. Section IV presents new upper capacity bounds for different categories of MIMO systems. In Section V, we focus on the tightness of the proposed bound while the numerical results are given in Section VI. Finally, Section VII summarizes the key findings.

## II. NOTATION AND DEFINITIONS

### A. Notation

We use upper and lower case boldfaces to denote matrices and vectors, respectively while the symbol  $\mathbb{C}$  denotes the set of complex-valued numbers. The nomenclature  $\sim \mathcal{CN}_{m,n}(\mathbf{A}, \mathbf{B})$  stands for a  $(m \times n)$  complex normally distributed matrix with mean  $\mathbf{A}$  and covariance  $\mathbf{B}$ . The entries of a  $(m \times n)$  matrix  $\mathbf{A}$  are denoted as  $\{\mathbf{A}\}_{i,j}$  where  $i = 1, \dots, m$  and  $j = 1, \dots, n$ . An  $(m \times m)$  identity matrix is expressed as  $\mathbf{I}_m$  while the all-zero  $(m \times n)$  matrix as  $\mathbf{0}_{m \times n}$ . The symbols  $(\cdot)^T$ ,  $(\cdot)^H$  and  $(\cdot)^{-1}$  correspond to transposition, Hermitian transposition and matrix inversion whereas  $\otimes$  is the Kronecker product; henceforth, we will use  $\det$  and  $|\cdot|$  to interchangeably denote the determinant operator while  $\|\cdot\|_F$  will return the Frobenius norm of a matrix. Finally,  $\text{etr}(\cdot)$  is a shorthand notation for  $\exp(\text{tr}(\cdot))$ .

### B. Multivariate Statistics Definitions

*Definition 1:* Let's assume that the  $(m \times n)$  complex matrix  $\mathbf{X}$ , with  $m \leq n$ , is distributed according to  $\mathbf{X} \sim \mathcal{CN}_{m,n}(\mathbf{M}, \Sigma \otimes \mathbf{I}_n)$ , where  $\Sigma \in \mathbb{C}^{m \times m}$  is a positive definite Hermitian matrix. Then, the matrix  $\mathbf{S} = \mathbf{X}\mathbf{X}^H$  follows the complex non-central Wishart distribution with  $n$  degrees of freedom and non-centrality matrix  $\Omega = \Sigma^{-1}\mathbf{M}\mathbf{M}^H$ , commonly denoted as  $\mathbf{S} \sim \mathcal{CW}_m(n, \Sigma, \Omega)$ . The probability density function (PDF) of a  $(m \times n)$  complex non-central Wishart matrix  $\mathbf{S}$  was given by James [24] as

$$f(\mathbf{S}) = \frac{\text{etr}(-\Omega)}{\tilde{\Gamma}_m(n) \det(\Sigma)^n} \det(\mathbf{S})^{n-m} \text{etr}(\Sigma^{-1}\mathbf{S}) {}_0\tilde{F}_1(n; \Omega \Sigma^{-1}\mathbf{S}) \quad (1)$$

where  $\tilde{\Gamma}_m(n)$  is the complex multivariate gamma function defined as

$$\tilde{\Gamma}_m(n) \triangleq \pi^{\frac{m(m-1)}{2}} \prod_{j=1}^m \Gamma(n-j+1) \quad (2)$$

with  $\Gamma(\cdot)$  being the standard gamma function and  ${}_0\tilde{F}_1(b, \mathbf{A})$  the complex Bessel hypergeometric function of one matrix argument of a Hermitian matrix  $\mathbf{A}$ .

*Definition 2:* Let's assume that the  $(m \times n)$  complex matrix  $\mathbf{X}$ , with  $m \leq n$ , is distributed according to  $\mathbf{X} \sim \mathcal{CN}_{m,n}(\mathbf{M}, \Sigma \otimes \Psi)$ , where  $\Sigma \in \mathbb{C}^{m \times m}$  and  $\Psi \in \mathbb{C}^{n \times n}$  are positive definite Hermitian matrices. Then, the matrix  $\mathbf{Q} = \mathbf{X}\mathbf{\Lambda}\mathbf{X}^H$ , with  $\mathbf{\Lambda} \in \mathbb{C}^{n \times n}$ , is said to be a non-central matrix-variate quadratic form denoted as  $\mathbf{Q} \sim \mathcal{CQ}_{m,n}(\mathbf{\Lambda}, \Sigma, \Psi, \mathbf{M})$ .

In [19] and [15], the PDF of  $\mathbf{Q}$  was expressed through complex Hayakawa polynomials of two matrix arguments which are very difficult to calculate numerically. A more tractable version of the associated PDF as a product of hypergeometric functions, can be found in [25, Eq. (5)]. Please note that non-central quadratic forms degenerate into non-central Wishart matrices when  $\Psi = \mathbf{I}_n$  and when either  $\mathbf{\Lambda} = \mathbf{I}_n$  or  $\mathbf{\Lambda}$  is idempotent with rank  $L \geq m$  [19], [26]. The following theorem returns the  $v$ th moment of the determinant of  $(2 \times 2)$  complex quadratic forms.

*Theorem 1:* Let  $\mathbf{Q} \sim \mathcal{CQ}_{2,2}(\mathbf{I}_2, \Sigma, \Psi, \mathbf{M})$ . Then, the  $v$ th moment of its determinant  $|\mathbf{Q}|$  is given by

$$E[|\mathbf{Q}|^v] = |\Sigma\Psi|^v \left[ \frac{\tilde{\Gamma}_2(v+2)}{\tilde{\Gamma}_2(2)} \right] {}_1\tilde{F}_1(-v; 2; -\Theta) \quad (3)$$

where  ${}_1\tilde{F}_1(a, b, \mathbf{A})$  is the hypergeometric function of a matrix argument,  $\Theta = \Psi^{-1}\bar{\mathbf{M}}\bar{\mathbf{M}}^H$  and  $\bar{\mathbf{M}} = \Sigma^{-1/2}\mathbf{M}$ .

*Proof:* A detailed proof is given in Appendix A. ■

We underline the fact that the theorem is applicable only to  $(2 \times 2)$  quadratic forms since for matrix sizes of  $(m \times n)$ , a finite summation over a collection of  $\binom{n}{m}$  subsets needs to take place. The interested readers are referred to [15] for a detailed discussion. A simplified formula can now be obtained for the first-order moment of the determinant after applying the determinant representation of the hypergeometric function. In particular,

*Corollary 1:* For  $v = 1$ , (3) reduces to

$$E[|\mathbf{Q}|] = 2|\Sigma\Psi| \left( 1 + \frac{1}{2}\text{tr}(\Theta) + \frac{1}{2}\det(\Theta) \right). \quad (4)$$

*Proof:* The authors in [19] showed that for any square matrix  $\mathbf{B} \in \mathbb{C}^{m \times m}$ , its hypergeometric function  ${}_1\tilde{F}_1(c; d; \mathbf{B})$  can be expressed according to

$${}_1\tilde{F}_1(c; d; \mathbf{B}) = \frac{\det\left({}_1\tilde{F}_1(c-m+j; d-m+j; b_i) b_i^{j-1}\right)}{\prod_{i < j} (b_j - b_i)} \quad (5)$$

where  $b_1, b_2, \dots, b_m$  is the set of non-zero eigenvalues of  $\mathbf{B}$ . After taking into account the following properties for the scalar hypergeometric functions

$${}_1\tilde{F}_1(-2, 1; z) = 1 - 2z + \frac{1}{2}z^2 \quad (6)$$

$${}_1\tilde{F}_1(-1, 2; z) = 1 - \frac{1}{2}z^2 \quad (7)$$

it is trivial to show that for the dual case under consideration

$${}_1\tilde{F}_1(-1; 2; -\Theta) = \frac{1}{2}(2 + \theta_1 + \theta_2 + \theta_1\theta_2) \quad (8)$$

where  $\theta_1, \theta_2$  are the eigenvalues of  $\Theta$ . The proof concludes after recalling that the sum and product of the eigenvalues return the trace and the determinant of a matrix, respectively. ■

It's noteworthy that exactly the same result can be drawn if we represent the hypergeometric function  ${}_1\tilde{F}_1(-1; 2; -\Theta)$  via its zonal polynomials, as originally proposed in [26] and amended for the MIMO case in [18, Appendix I].

### III. MIMO CHANNEL MODEL

#### A. Statistics of the channel matrix

As was previously highlighted, we are particularly interested in dual-branch MIMO configurations where both the Tx and Rx are equipped with two antenna elements and spatial correlation is also present at both ends. Under Ricean fading conditions, the channel transfer function matrix  $\mathbf{H}$  consists of a spatially deterministic specular component  $\mathbf{H}_L$  and a randomly distributed component  $\mathbf{H}_W$  which accounts for the scattered signals. Then, the underlying model for a double-sided correlated Rician MIMO channel reads as

$$\mathbf{H} = \sqrt{\frac{K}{K+1}}\mathbf{H}_L + \sqrt{\frac{1}{K+1}}\mathbf{R}_r^{1/2}\mathbf{H}_W\mathbf{R}_t^{1/2} \quad (9)$$

where  $K$  is the Ricean  $K$ -factor expressing the ratio of powers of the free-space signal and the scattered waves. The receive and transmit correlation matrices are respectively defined as

$$\mathbf{R}_r \triangleq E_{\mathbf{H}} \{ \mathbf{H}\mathbf{H}^H \}. \quad (10)$$

$$\mathbf{R}_t \triangleq E_{\mathbf{H}} \{ (\mathbf{H}^H\mathbf{H})^T \} \quad (11)$$

and are commonly taken to be Hermitian positive definite with unit diagonal entries<sup>1</sup>. Please note that we adopt this Kronecker-type of modelling, thanks to its inherent simplicity and the fact that is sufficiently

<sup>1</sup>This assumption originates from [28] where it was illustrated that the elements of  $\mathbf{H}$  are essentially samples of a two-dimensional stationary random field and its diagonal entries correspond to the constant power in the spatial field.

accurate when a small number of antenna is used [29]. Besides, it has been extensively used in the corresponding literature to model the correlated structure of most MIMO systems, as for instance in [4], [16], [19]. The entries of  $\mathbf{H}_W$  are commonly modeled as i.i.d. zero-mean, unit variance complex Gaussian random variables and under these circumstances the channel matrix is distributed according to

$$\mathbf{H} \sim \mathcal{CN}_{2,2} \left( \sqrt{K/(K+1)} \mathbf{H}_L, (K+1)^{-1} \mathbf{R}_r \otimes \mathbf{R}_t \right). \quad (12)$$

Throughout this paper, our purpose is to compare the MIMO gains of different configurations and therefore the capacities should be analyzed independently of the average SNR. This is achieved by normalizing the channel matrices so that following constraint is fulfilled

$$E [\|\mathbf{H}\|_F^2] = E [\text{tr}(\mathbf{H}\mathbf{H}^H)] = 4. \quad (13)$$

We recall that the key normalization in (13) has been widely adopted into the capacity characterization of MIMO systems [1], [2], [9], [18]. From a physical viewpoint, the path-loss effects are removed and the system is assumed to have perfect power control.

### B. Geometrical LoS MIMO configurations

Referring back to (9), we can now examine the structure of the LoS matrix component. In free-space, the complex entries of  $\mathbf{H}_L$  are of the form  $e^{-jkd_{m,n}}/d_{m,n}$ , where  $k = 2\pi/\lambda$  is the wavenumber corresponding to the carrier wavelength  $\lambda$  and  $d_{m,n}$  is the distance between a receive element  $m \in \{1, 2\}$  and a transmit element  $n \in \{1, 2\}$ . Please note that we have assumed, without loss of generality, isotropic radiators and negligible differences in the path-losses. Then, we can write

$$\mathbf{H}_L = \begin{bmatrix} e^{-jkd_{1,1}} & e^{-jkd_{1,2}} \\ e^{-jkd_{2,1}} & e^{-jkd_{2,2}} \end{bmatrix}. \quad (14)$$

From a geometrical viewpoint, a side view of the MIMO system under investigation is depicted in Fig. 1, where both ends employ 2-element Uniform Linear Arrays (ULAs) and the distance between the first element of each array is  $D$ . The inter-element spacings are respectively  $s_1$  (Tx) and  $s_2$  (Rx). An axis rotation by an angle  $\theta$  has been conducted around the  $y$  axis in order to make the array origins lie on the same axis and ease the post-processing.

In the following, we explore two different LoS configurations, namely a LR and an optimized HR configuration. The former represents any conventional architecture with inter-element spacings of the order of wavelength and arrays in the far-field region; this means that the LoS signals are basically plane wavefronts which inherently suffer from excessive spatial correlation between their rays phases. These

architectures offer a minimal spatial multiplexing gain since the transmitted LoS signals impinging on the Rx carry almost identical spatial characteristics and therefore their differentiation is difficult and susceptible to unavoidable detection errors.

The latter configuration, however, belongs in a family of specifically designed full-rank LoS configurations which deliberately assign unique spatial signatures on the received signals by inserting a phase difference of  $\pi/2$  between them [21]–[23]. This is achieved by appropriately positioning the antenna elements at both ends of the link, so that the LoS signals propagate as spherical wavefronts in the near-field of the arrays. By doing so, subchannel orthogonality, which is a key condition for capacity maximization, is achieved and two equal LoS eigenvalues are eventually obtained while the systems delivers an enhanced MIMO capacity in the presence of strong direct components. For the assumed model, the optimum inter-element spacings were derived in [23]

$$s_1 = s_2 = s_{opt} \approx \sqrt{\frac{\lambda D}{2 \cos^2 \theta}}. \quad (15)$$

We note that for optimized configurations the effects of spatial correlation are rather weak due to the increased antenna spacings. However, in the following analysis the presence of correlation is considered for the fairness of comparison with conventional configurations.

#### IV. ERGODIC CAPACITY UPPER BOUNDS

In this section, novel expressions for the upper bound of ergodic capacity based on a power constraint are derived. Let's assume firstly that the Rx has perfect CSI while the Tx knows neither the statistics nor the instantaneous CSI. In this case, a sensible choice for the Tx is to split the total amount of power equally among all data streams and, consequently, an equal-power transmission scheme takes place. The justification for adopting this scheme, though not optimal, originates from the so-called “maxmin” property [30] which demonstrated the robustness of the above mentioned technique for maximizing the capacity of the worst fading correlation matrix [8]. Under these circumstances, the ergodic ( $2 \times 2$ ) MIMO capacity (in bits/s/Hz), is given by the following well-known relationship [1], [2]

$$\bar{C} = E \left[ \log_2 \left( \det \left( \mathbf{I}_2 + \frac{\rho}{2} \mathbf{H} \mathbf{H}^H \right) \right) \right] \quad (16)$$

where the expectation is taken across all the random realizations of  $\mathbf{H}$  while  $\rho$  denotes the SNR per receiver branch.

### A. Double-sided correlated Ricean and Rayleigh fading

In the general case of double-sided correlated Ricean fading, where the channel matrix is distributed according to (12), the instantaneous MIMO correlation matrix  $\widetilde{\mathbf{W}} = \mathbf{H}\mathbf{H}^H$  exhibits non-central quadratic form distribution with the following properties

$$\widetilde{\mathbf{W}} \sim \mathcal{CQ}_{2,2} \left( \mathbf{I}_2, \mathbf{R}_r / (K + 1), \mathbf{R}_t, \sqrt{K / (K + 1)} \mathbf{H}_L \right). \quad (17)$$

The following theorem returns an upper bound on the ergodic capacity of a double-sided correlated dual MIMO Ricean system.

*Theorem 2:* The ergodic capacity in bits/s/Hz of a  $(2 \times 2)$  double-sided correlated MIMO Ricean channel with mean matrix  $\sqrt{\frac{K}{K+1}} \mathbf{H}_L$ , receive correlation matrix  $(K + 1)^{-1} \mathbf{R}_r$  and transmit correlation matrix  $\mathbf{R}_t$ , is analytically upper bounded by

$$\overline{C} \leq \log_2 \left( 1 + 2\rho + \frac{\gamma\rho^2}{2} \right) \quad (18)$$

where the parameter  $\gamma$  is given as

$$\gamma = (K + 1)^{-2} |\mathbf{R}_r| |\mathbf{R}_t| \left( 1 + \frac{1}{2} \text{tr}(\boldsymbol{\Theta}) + \frac{1}{2} \det(\boldsymbol{\Theta}) \right) \quad (19)$$

with

$$\boldsymbol{\Theta} = K \mathbf{R}_t^{-1} \mathbf{R}_r^{-1/2} \mathbf{H}_L \mathbf{H}_L^H \left( \mathbf{R}_r^{-1/2} \right)^H. \quad (20)$$

*Proof:* An alternative way to express the ergodic MIMO capacity is through the real positive eigenvalues  $\tilde{w}_1, \tilde{w}_2$  of  $\widetilde{\mathbf{W}}$  which, in practice, represent the power carried by each spatial subchannel. Then, (16) can be rewritten as

$$\overline{C} = E \left[ \log_2 \left( 1 + \frac{\rho}{2} \tilde{w}_1 \right) \left( 1 + \frac{\rho}{2} \tilde{w}_2 \right) \right]. \quad (21)$$

If we expand (21), we can easily get

$$\overline{C} = E \left[ \log_2 \left( 1 + \frac{\rho}{2} (\tilde{w}_1 + \tilde{w}_2) + \frac{\rho^2}{4} \det(\widetilde{\mathbf{W}}) \right) \right]. \quad (22)$$

Taking into account that  $\log(\cdot)$  is a concave function and making use of the Jensen's inequality we obtain

$$\begin{aligned} \overline{C} &\leq \log_2 \left( 1 + \frac{\rho}{2} E[\tilde{w}_1 + \tilde{w}_2] + \frac{\rho^2}{4} E[\det(\widetilde{\mathbf{W}})] \right) \\ &= \log_2 \left( 1 + 2\rho + \frac{\rho^2}{4} E[\det(\widetilde{\mathbf{W}})] \right). \end{aligned} \quad (23)$$

The second line follows from the power constraint in (13), or equivalently

$$E [\text{tr}(\mathbf{H}\mathbf{H}^H)] = E [\text{tr}(\widetilde{\mathbf{W}})] = E [\tilde{w}_1 + \tilde{w}_2] = 4. \quad (24)$$

The upper bound in (18) follows immediately after introducing Corollary 1 and simplifying.  $\blacksquare$

With regard to the novel upper bound derived in (18), two important remarks should be made. The first one is that the bound is strictly applicable to dual-branch configurations since for larger MIMO setups, we end up with a series of eigenvalue cross-products that are created after expanding (21). Secondly, by inspection of (18), it can be inferred that the proposed upper bound is rather simple as it just requires the computation of the elementary functions of three different deterministic matrices ( $\mathbf{R}_r$ ,  $\mathbf{R}_t$  and  $\Theta$ ) only once. Comparatively, the bound in [19, Eq. (66)] for arbitrary rank of the LoS component, relies on an infinite summation of Hayakawa polynomials and therefore is hard to evaluate either analytically or numerically.

In the case of double-sided correlated Rayleigh fading ( $K = 0$ ), the channel matrix is distributed according to  $\mathbf{H} \sim \mathcal{CN}_{2,2}(\mathbf{0}_2, \mathbf{R}_r \otimes \mathbf{R}_t)$  and the upper bound in (18) reduces to

$$\bar{C} \leq \log_2 \left( 1 + 2\rho + \frac{\rho^2}{2} |\mathbf{R}_r \mathbf{R}_t| \right) \quad (25)$$

which is in perfect agreement with the bound derived in [4, Eq. (25)].

### B. Uncorrelated Ricean and Rayleigh fading

For the sake of brevity, the case of single-side correlation is omitted in this paper since the derivation is based on exactly the same concept as before. Therefore, we now consider the special case of both ends exhibiting uncorrelated i.i.d. Ricean fading. Under these circumstances, the channel matrix is distributed according to

$$\mathbf{H} \sim \mathcal{CN}_{2,2} \left( \sqrt{\frac{K}{K+1}} \mathbf{H}_L, \frac{1}{K+1} \mathbf{I}_2 \otimes \mathbf{I}_2 \right). \quad (26)$$

*Corollary 2:* The ergodic capacity in bits/s/Hz of a  $(2 \times 2)$  uncorrelated MIMO Ricean channel with mean matrix  $\sqrt{\frac{K}{K+1}} \mathbf{H}_L$  and receive correlation matrix  $\mathbf{R}_r = \frac{1}{K+1} \mathbf{I}_2$  is analytically upper bounded by

$$\bar{C} \leq \log_2 \left( 1 + 2\rho + \frac{\beta \rho^2}{2} \right) \quad (27)$$

where  $\beta = (1 + 2K + 0.5K^2 \det(\mathbf{T})) / (K+1)^2$  and  $\mathbf{T} = \mathbf{H}_L \mathbf{H}_L^H$ .

*Proof:* This corollary is a direct consequence of (18) after taking into account that  $\Theta \equiv K\mathbf{T}$  for the case of uncorrelated fading at both ends. Furthermore, it holds that  $\text{tr}(K\mathbf{T}) = K\text{tr}(\mathbf{T})$  and given that the entries of the deterministic LoS component matrix are unit-amplitude complex exponentials, it is trivial

to show that  $\text{tr}(\mathbf{T}) = 4$ . Likewise, the determinant of  $K\mathbf{T}$  may be expressed as  $\det(K\mathbf{T}) = K^2 \det(\mathbf{T})$  which concludes the proof. ■

The case of i.i.d. Rayleigh fading is obtained directly from (9), by setting  $K = 0$  and  $\mathbf{R}_r = \mathbf{R}_t = \mathbf{I}_2$ . The upper bound in (27) then reduces to ( $\beta = 1$ )

$$\bar{C} \leq \log_2 \left( 1 + 2\rho + \frac{\rho^2}{2} \right) \quad (28)$$

which is identical with the results presented in [18, Eq. (5)], [3, Theorem 2] and [4, Eq. (22)].

## V. TIGHTNESS OF THE UPPER BOUND

In this section, we show that the upper bound converges to the true capacity at low SNRs whereas at high SNRs, the offset from the true capacity is analytically determined. In general, the absolute error  $\epsilon$  inserted by an upper bound  $U$  is given as  $\epsilon = U - \bar{C}$ .

*Corollary 3:* The upper bound in (18) becomes asymptotically tight as the SNR tends to zero.

*Proof:* We begin with further upper bounding the ergodic capacity in (18) according to

$$\bar{C} \leq \frac{1}{\ln 2} \left( 2\rho + \frac{\gamma\rho^2}{2} \right) \quad (29)$$

where we have made use of the property  $\ln(1+x) \leq x$ . Following [18] and [31], we can lower bound the ergodic capacity according to [31, Eq. (23)]

$$\begin{aligned} \bar{C} &\geq E \left[ \log_2 \left( 1 + \frac{\rho}{2} \|\mathbf{H}\|_F^2 \right) \right] \\ &\geq \frac{\rho}{2 \ln 2} E \left[ \|\mathbf{H}\|_F^2 \right] - \frac{1}{2 \ln 2} \left( \frac{\rho}{2} \right)^2 E \left[ \|\mathbf{H}\|_F^4 \right] \\ &= \frac{2\rho}{\ln 2} - \frac{\rho^2}{8 \ln 2} E \left[ \|\mathbf{H}\|_F^4 \right]. \end{aligned} \quad (30)$$

The second line follows from the property  $\ln(1+x) \geq x - \frac{1}{2}x^2$ . We can now subtract (30) from (29) and then the absolute error  $\epsilon$  of the proposed upper bound becomes

$$\epsilon = \frac{\rho^2}{2 \ln 2} \left( \gamma + \frac{1}{4} E \left[ \|\mathbf{H}\|_F^4 \right] \right) \quad (31)$$

which asymptotically tends to zero as  $\rho \rightarrow 0$ . ■

*Corollary 4:* As the SNR  $\rho \rightarrow \infty$ , the absolute error inserted by the upper bound in (18) tends to

$$\epsilon = \log_2(2\gamma) - E \left[ \log_2 \left( \det \left( \widetilde{\mathbf{W}} \right) \right) \right]. \quad (32)$$

*Proof:* As  $\rho \rightarrow \infty$ , the upper bound  $U$  in (18), simplifies to

$$U \approx \log_2(2\gamma) + 2 \log_2 \left( \frac{\rho}{2} \right). \quad (33)$$

In (21), the quadratic term becomes significantly larger in the high SNR-regime and therefore the ergodic capacity may be approximated as

$$\begin{aligned}\bar{C} &\approx E \left[ \log_2 \left( \frac{\rho^2}{4} \det(\widetilde{\mathbf{W}}) \right) \right] \\ &= 2 \log_2 \left( \frac{\rho}{2} \right) + E \left[ \log_2 \left( \det(\widetilde{\mathbf{W}}) \right) \right].\end{aligned}\quad (34)$$

Subtracting (34) from (33), yields (32). ■

From the above equation, it is apparent that the bound's error is given in a non-analytical form; in this light, the crucial issue is to determine the expectation of the logdet function of a complex non-central quadratic matrix, which involves a nonlinear log function.

*Theorem 3:* Let's assume that  $\widetilde{\mathbf{W}} \sim \mathcal{CQ}_{2,2} \left( \mathbf{I}_2, \mathbf{R}_r / (K+1), \mathbf{R}_t, \sqrt{K/(K+1)} \mathbf{H}_L \right)$ . Then the first-order moment of the logarithm of its determinant is given as

$$\begin{aligned}E \left[ \log_2 \left( \det(\widetilde{\mathbf{W}}) \right) \right] &= \frac{1}{\ln 2} \left[ \psi(1) + \psi(2) - 2 \ln(K+1) + \ln |\mathbf{R}_r \mathbf{R}_t| \right. \\ &\quad \left. - \frac{1}{\theta_1 - \theta_2} (\Lambda_1(\Theta) + \Lambda_2(\Theta)) \right]\end{aligned}\quad (35)$$

where  $\theta_1, \theta_2$  are the eigenvalues of the matrix  $\Theta$  which was given in (20) while the well-known digamma functions  $\psi(x)$  are defined as

$$\psi(x) \triangleq \frac{d}{dx} \ln \Gamma(x) = \frac{\Gamma'(x)}{\Gamma(x)}.\quad (36)$$

The polynomial terms  $\Lambda_1(\Theta)$  and  $\Lambda_2(\Theta)$  are essentially functions of the eigenvalues  $\theta_1$  and  $\theta_2$  and, in particular

$$\Lambda_1(\Theta) = \theta_2 h_1(\theta_1) - h_2(\theta_1)\quad (37)$$

$$\Lambda_2(\Theta) = h_2(\theta_2) - \theta_1 h_1(\theta_2)\quad (38)$$

where

$$h_1(x) = \sum_{k=0}^{\infty} \frac{\mathcal{P}(k, x)}{k}\quad (39)$$

$$h_2(x) = x \sum_{k=0}^{\infty} \frac{\mathcal{P}(k, x)}{k+1}\quad (40)$$

with  $\mathcal{P}(a, x)$  being the regularized gamma function [32, 6.5.1].

*Proof:* A detailed proof is given in Appendix B. ■

Please note that the derivation of this formula relies, without loss of generality, on the assumption of two non-zero eigenvalues of the matrix  $\Theta$ . For the case of rank-1 matrices, a similar analysis should be

followed; this is however beyond the scope of the paper and the interested readers are referred to [19] for a thorough discussion. Evidently, after replacing (35) into (32), we can obtain an analytical formula for the bound's offset at high SNRs, for the general case of double-sided correlated Ricean fading. Most importantly, this result can be further used to deduce exact capacity expressions in the high-SNR regime.

When the channel exhibits i.i.d. Ricean fading and both ends are employed with optimally designed arrays as discussed in Section III-B, the LoS component yields two equal eigenvalues and thus, the following corollary should be introduced.

*Corollary 5:* As the SNR  $\rho \rightarrow \infty$ , the absolute error inserted by the upper bound for the case of i.i.d. Ricean fading and optimized LoS configurations tends to

$$\epsilon = \log_2(2\beta) - \frac{1}{\ln 2} \left[ \psi(1) + \psi(2) - 2 \ln(K+1) + \sum_{k=1}^{\infty} \frac{(2k+1)\gamma(k, \omega) - \omega e^{-\omega} \omega^{k-1}}{(k+1)!} \right] \quad (41)$$

where  $\omega = \omega_1 = \omega_2$  represents any of the two equal eigenvalues of  $\mathbf{\Omega} \equiv K\mathbf{T}$  and  $\gamma(a, x) = \int_0^x t^{a-1} e^{-t} dt$  is the lower incomplete gamma function.

*Proof:* The proof starts by noting that for i.i.d. Ricean fading  $\Theta$  should be replaced by  $\mathbf{\Omega} \equiv K\mathbf{T}$  in all manipulations. Further, in the specific case of optimized configurations, the equality of eigenvalues leads to a division by zero in (35). In order to circumvent this singularity, we employ *de l'Hôpital's* rule to get a solution at the limit ( $\omega_1 \rightarrow \omega_2$ ). In particular, the last term in (35) can be rewritten as

$$\xi = \lim_{\varepsilon \rightarrow 0} \left[ \frac{d}{d\varepsilon} (\omega h_1(\omega + \varepsilon) - h_2(\omega + \varepsilon)) - h_1(\omega) \right]. \quad (42)$$

Taking into account that

$$\frac{d}{dx} \mathcal{P}(a, x) = \frac{e^{-x} x^{a-1}}{\Gamma(a)} \quad (43)$$

and after some algebraic manipulations we end up with

$$\lim_{\varepsilon \rightarrow 0} \frac{d}{d\varepsilon} h_1(\omega + \varepsilon) = \sum_{k=1}^{\infty} \frac{e^{-\omega} \omega^{k-1}}{k\Gamma(k)} \quad (44)$$

$$\lim_{\varepsilon \rightarrow 0} \frac{d}{d\varepsilon} h_2(\omega + \varepsilon) = \sum_{k=1}^{\infty} \frac{e^{-\omega} \omega^{k-1}}{(k+1)\Gamma(k)} + \frac{h_2(\omega)}{\omega}. \quad (45)$$

Substituting (44)–(45) into (42), factorizing and simplifying yields (41). ■

## VI. NUMERICAL RESULTS

In this section, the theoretical analysis presented in Sections IV and V is validated through a set of Monte-Carlo simulations. Assuming a carrier frequency of 5.9 GHz,  $D = 5.3852$  m and  $\theta = 21.80^\circ$  the

optimum inter-element spacings via (15) are  $s_1 = s_2 = 39.85$  cm ( $7.83\lambda$ ) whereas for the conventional configuration the spacings become  $s_1 = s_2 = 2.54$  cm ( $0.5\lambda$ ). The LoS matrix components are given as

$$\mathbf{H}_L^{opt} = \begin{bmatrix} 0.8384 + j0.5451 & 0.9074 - j0.4202 \\ 0.0160 - j0.9999 & 0.8384 + j0.5451 \end{bmatrix}. \quad (46)$$

$$\mathbf{H}_L^{conv} = \begin{bmatrix} 0.8384 + j0.5451 & 0.8272 - j0.5618 \\ -0.1653 + j0.9862 & 0.8384 + j0.5451 \end{bmatrix} \quad (47)$$

with the Los eigenvalues of  $\mathbf{T}$  being equal to  $(2, 2)$  and  $(4, 4.08 \times 10^{-5})$ , respectively. Please note that, in practice, we simulate a system suitable for Dedicated Short Range Communications (DSRC) which have recently emerged to provide a plethora of safety on-the-road applications; a supporting protocol has also been developed for the case of Intelligent Transportation Systems (ITS), that is the IEEE 802.11p protocol [33].

Throughout the simulations, we adopt the widely used constant correlation model thanks to its inherent simplicity. In this context, the entries of  $\mathbf{R}_r$  and  $\mathbf{R}_t$  in (9) can be modeled as  $\{\mathbf{R}_r\}_{i,j} = (\delta_R)^{|i-j|}$  and, in analogy,  $\{\mathbf{R}_t\}_{i,j} = (\delta_T)^{|i-j|}$ , where  $\delta_R, \delta_T \in [0, 1)$ . After generating 50,000 Monte-Carlo realizations of the channel matrix according to (9) and setting  $\delta_R = 0.2$  and  $\delta_T = 0.5$ , the proposed bound in (18) is firstly evaluated against the operating SNR for different values of the  $K$ -factor. From Figs. 2(a) and 2(b), it can be easily seen that the bound is remarkably tight for the optimized configuration and, likewise, performs satisfactorily for conventional configurations. As anticipated, in the low-SNR regime both bounds converge asymptotically to the empirical values of ergodic capacity. Generally speaking, the bound becomes tighter as  $K$  increases and SNR decreases which is line with the conclusions in [14], [16], [18]. Most importantly, ergodic capacity benefits from the presence of strong non-fading components when both ends are equipped with specifically designed arrays. This is a result of the two orthogonal LoS MIMO subchannels, as was initially demonstrated in [21]–[23] and contradicts the common belief that higher  $K$ -factors always result in a decrease in MIMO capacity since the beneficial effects of scattering are cancelled [11], [12], [14].

As a next step, the effects of the  $K$ -factor on the performance of the proposed bound are investigated in Fig. 3, where it is again apparent that both bounds become tighter with an increasing  $K$ -factor. For Rayleigh-fading conditions though, or  $K \leq 0$  dB, the achieved tightness is degraded and, under these circumstances, it is sensible to use more efficient bounds which are inherently tied to Rayleigh channels, like the ones presented in [3]–[5]. Once more, the superiority of the optimized configurations is illustrated as  $K$  gets larger whereas in the limit ( $K \rightarrow \infty$ ), conventional configurations degenerate into a single-path

link. On the other hand, for  $K \leq 0$  dB the advantages of optimized configurations diminish and in the limit ( $K \rightarrow -\infty$  dB) the LoS component vanishes and we end up with a pure i.i.d. Rayleigh channel.

In Fig. 4, the relationship between practical values of spatial correlation and MIMO capacity is addressed. Clearly, the effects of correlation on ergodic capacity become less significant (smaller dynamic range) as the  $K$ -factor gets higher for both configurations under investigation, i.e. high  $K$ -factors provide robustness against spatial correlation. As expected, the large inter-element spacings make the optimized setup remain unaffected by the level of correlation; hence, it offers almost the same ergodic capacity regardless of the values of  $\delta_R$  and  $\delta_T$ . The conventional configuration, however, suffers from spatial correlation with the ergodic capacity decreasing as correlation gets higher. Intuitively, the tightness of the corresponding bound is relatively improved in the high-correlation regime. Please note that this outcome is in agreement with the results given in [4], [16], [18].

At the last stage of the evaluation process, we consider the high-SNR deviation between the ergodic capacity and the proposed upper bound using the closed-form formulae in (32) and (35). In Fig. 5, these analytical curves are overlaid with the outputs of a Monte-Carlo simulator with the match being remarkably good. The error associated with optimized configurations is systematically lower than that of conventional ones, as a result of the rank-deficiency of the former. What's more, it appears that the latter error has a much smaller dynamic range revealing that a high  $K$ -factor does not have an extensive impact on its value. On the other hand, the bound for the optimized configuration yields an enhanced tightness as  $K$  increases and under strong Ricean conditions, its absolute error is minimized.

## VII. CONCLUSION

In this paper, we considered the derivation of a tractable upper bound for the ergodic capacity of dual-branch MIMO Ricean systems with the key concept originating from a widely used power constraint. The proposed bound depends merely on the SNR and the expected value of the determinant of either a non-central quadratic form or, in special cases, a non-central Wishart matrix. The main advantage of this novel bound is its simplicity and the fact that it is not confined to the common case of rank-1 deterministic LoS components. For the sake of completeness, we explored two different classes of LoS configurations, these are a conventional and an optimized architecture which benefits from the presence of strong deterministic components by offering two equal LoS eigenvalues. It was demonstrated that the bound is remarkably tight for the optimized case and marginally looser for the conventional setups. The tightness of the bound was finally assessed in the low and high-SNR regions; in the former, the bound becomes asymptotically tight whereas in the latter, the absolute error tends to a constant value that was

analytically determined and validated through Monte-Carlo simulations.

## APPENDIX A

### PROOF OF THEOREM 1

We begin by expressing the determinant of the quadratic form  $\mathbf{Q} \sim \mathcal{CQ}_{2,2}(\mathbf{I}_2, \boldsymbol{\Sigma}, \boldsymbol{\Psi}, \mathbf{M})$  as

$$\begin{aligned} E [\det(\mathbf{Q})^v] &= E \left[ \det(\mathbf{X}\mathbf{X}^H)^v \right] \\ &= E \left[ \det \left( \boldsymbol{\Sigma}^{1/2} \bar{\mathbf{X}} \bar{\mathbf{X}}^H \boldsymbol{\Sigma}^{1/2} \right)^v \right] \\ &= \det(\boldsymbol{\Sigma})^v E \left[ \det(\bar{\mathbf{X}} \bar{\mathbf{X}}^H)^v \right] \end{aligned} \quad (48)$$

where the complex normal matrix  $\bar{\mathbf{X}}$  is distributed according to

$$\mathbf{X} \sim \mathcal{CN}_{2,2}(\bar{\mathbf{M}}, \mathbf{I}_2 \otimes \boldsymbol{\Psi}). \quad (49)$$

Using a result from [15] through the aid of the Cauchy-Binet formula, we can show that

$$\bar{\mathbf{X}}^H \bar{\mathbf{X}} \sim \mathcal{CW}_2(2, \boldsymbol{\Psi}, \boldsymbol{\Theta}) \quad (50)$$

and the expectation of the determinant in (48) can now be evaluated through [19, Theorem 1] to obtain

$$E \left[ \det(\bar{\mathbf{X}} \bar{\mathbf{X}}^H)^v \right] = \det(\boldsymbol{\Psi})^v \left[ \frac{\tilde{\Gamma}_2(v+2)}{\tilde{\Gamma}_2(2)} \right] \text{etr}(\boldsymbol{\Theta}) {}_1\tilde{F}_1(v+2; 2; \boldsymbol{\Theta}) \quad (51)$$

where we have made use of the following property for the determinant of the product of square matrices

$$\det(\mathbf{CD}) = \det(\mathbf{DC}). \quad (52)$$

The proof concludes after introducing the well-known Kummer relation for hypergeometric functions of one matrix argument [34]

$${}_1\tilde{F}_1(a; b; \mathbf{S}) = \text{etr}(\mathbf{S}) {}_1\tilde{F}_1(b-a; b; -\mathbf{S}) \quad (53)$$

## APPENDIX B

### PROOF OF THEOREM 3

The proof begins with the following key transformation

$$E[\ln x] = \frac{d}{dv} E[x^v] \Big|_{v=0} \quad (54)$$

which holds since, by definition,  $x^v = e^{v \ln x}$ . By combining (54) and (3) and denoting

$$\zeta = E \left[ \log_2 \left( \det(\tilde{\mathbf{W}}) \right) \right] = \frac{1}{\ln 2} E \left[ \ln \left( \det(\tilde{\mathbf{W}}) \right) \right] \quad (55)$$

we can directly get

$$\zeta = \frac{1}{\ln 2} \frac{d}{dv} \left\{ |(K+1)^{-1} \mathbf{R}_r \mathbf{R}_t|^v \left[ \frac{\tilde{\Gamma}_2(v+2)}{\tilde{\Gamma}_2(2)} \right] {}_1\tilde{F}_1(-v; 2; -\Theta) \right\} \Big|_{v=0}. \quad (56)$$

We can easily observe that the above differentiation consists of three multiplicative terms. Treating each one separately due to the chain rule, it is trivial to show that the first term results in  $\ln |\mathbf{R}_r \mathbf{R}_t| - 2 \ln(K+1)$ .

The second one, may be rearranged according to

$$\begin{aligned} \frac{d}{dv} \left\{ \frac{\tilde{\Gamma}_2(v+2)}{\tilde{\Gamma}_2(2)} \right\} \Big|_{v=0} &= \frac{\tilde{\Gamma}_2(v+2)}{\tilde{\Gamma}_2(2)} \frac{d}{dv} \left\{ \ln(\tilde{\Gamma}_2(v+2)) \right\} \Big|_{v=0} \\ &= \frac{d}{dv} \left\{ \sum_{i=1}^2 \ln(\Gamma(v+2-i+1)) \right\} \Big|_{v=0} \end{aligned} \quad (57)$$

which, after invoking the definition of digamma functions (36), readily yields  $\psi(1) + \psi(2)$ . Focusing now on the last term, we get

$$\begin{aligned} \frac{d}{dv} \left\{ {}_1\tilde{F}_1(-v; 2; -\Theta) \right\} \Big|_{v=0} &= \frac{d}{dv} \left\{ \text{etr}(-\Theta) {}_1\tilde{F}_1(v+2; v+2; \Theta) \right\} \Big|_{v=0} \\ &= \frac{\frac{d}{dv} {}_1\tilde{F}_1(v+2; v; \Theta) \Big|_{v=0}}{{}_1\tilde{F}_1(v; v; \Theta)}. \end{aligned} \quad (58)$$

where the second line follows from the property  ${}_1\tilde{F}_1(\alpha; \alpha; x) = \exp(x)$ . The proof concludes after introducing a very useful result from [19, Appendix II] for the nominator in the above equation. Substituting (57) and (58) into (56) and simplifying yields (35).

#### ACKNOWLEDGMENT

The first three authors would like to acknowledge the support of the Scottish Funding Council for the Joint Research Institute with Heriot-Watt University which is a part of the Edinburgh Research Partnership.

#### REFERENCES

- [1] I. E. Telatar, "Capacity of multi-antenna Gaussian channels," *ATT-Bell Labs Internal Technical Memorandum*, June 1995.
- [2] G. J. Foschini, "Layered space-time architecture for wireless communications in a fading environment when using multiple antennas," *Bell Labs Technical Journal*, vol. 1, no. 2, pp. 41–59, Autumn 1996.
- [3] A. Grant, "Rayleigh fading multi-antenna channels," *EURASIP Journal on Applied Signal Processing (Special Issue on Space-Time Coding (Part I))*, vol. 2002, no. 3, pp. 316–329, March 2002.
- [4] H. Shin and J. H. Lee, "Capacity of multi-antenna fading channels: Spatial fading correlation, double scattering, and keyhole," *IEEE Transactions on Information Theory*, vol. 49, no. 10, pp. 2636–2647, October 2003.

- [5] Q. T. Zhang, X. W. Cui and X. M. Li, "Very tight capacity bounds for MIMO-correlated Rayleigh-fading channels," *IEEE Transactions on Wireless Communications*, vol. 4, no. 2, pp. 681–688, March 2005.
- [6] J. Hansen and H. Bölcskei, "A geometrical investigation of the rank-1 Rician MIMO channel at high-SNR," in *Proc. International Symposium on Information Theory (ISIT)*, Chigano, USA, June 2004, p. 64.
- [7] G. Alfano, A. Lozano, A. M. Tulino, and S. Verdù, "Mutual information and eigenvalue distribution of MIMO Rician channels," in *Proc. International Symposium on Information Theory and Applications (ISITA)*, Parma, Italy, October 2004, pp. 1040–1045.
- [8] M. Kang and M. -S. Alouini, "Capacity of MIMO Rician channels," *IEEE Transactions on Wireless Communications*, vol. 5, no. 1, pp. 112–122, January 2006.
- [9] S. K. Jayaweera and H. V. Poor, "On the capacity of multiple-antenna systems in Rician fading," *IEEE Transactions on Wireless Communications*, vol. 4, no. 3, pp. 1102–1111, May 2005.
- [10] Y. -H. Kim and A. Lapidoth, "On the log determinant of non-central Wishart matrices," in *Proc. International Symposium on Information Theory (ISIT)*, Yokohama, Japan, June 2003, p. 54.
- [11] S. Jin and X. Gao, "Tight lower bounds on the ergodic capacity of Rician fading MIMO channels," in *Proc. International Conference on Communications (ICC)*, vol. 4, May 2005, pp. 2412–2416.
- [12] S. Jin and X. Gao, "Tight upper bound on the ergodic capacity of the Rician fading MIMO channels," in *Proc. Wireless Communications and Networking Conference (WCNC)*, vol. 1, March 2005, pp. 402–407.
- [13] M. R. McKay and I. B. Collings, "On the capacity of frequency-flat and frequency-selective Rician MIMO channels with single-sided correlation," *IEEE Transactions on Wireless Communications*, vol. 5, no. 8, pp. 2038–2043, August 2005.
- [14] X. W. Cui, Q. T. Zhang, and Z. M. Feng, "Generic procedure for tightly bounding the capacity of MIMO correlated Rician fading channels," *IEEE Transactions on Communications*, vol. 53, no. 5, pp. 890–898, May 2005.
- [15] M. R. McKay, P. J. Smith and I. B. Collings, "New properties of complex noncentral quadratic forms and bounds on MIMO mutual information," in *Proc. International Symposium on Information Theory (ISIT)*, Seattle, USA, July 2006, pp. 1209–1213.
- [16] S. Jin, X. Gao and X. You, "On the ergodic capacity of rank-1 Rician-fading MIMO channels," *IEEE Transactions on Information Theory*, vol. 53, no. 2, pp. 502–517, February 2007.
- [17] M. R. McKay and I. B. Collings, "Improved general lower bound for spatially-correlated Rician MIMO capacity," *IEEE Communications Letters*, vol. 10, no. 3, pp. 162–164, March 2006.
- [18] J. Salo, F. Mikas, and P. Vainikainen, "An upper bound on the ergodic mutual information in Rician fading MIMO channels," *IEEE Transactions on Wireless Communications*, vol. 5, no. 6, pp. 1415–1421, June 2006.
- [19] M. R. McKay and I. B. Collings, "General capacity bounds for spatially correlated Rician MIMO channels," *IEEE Transactions on Information Theory*, vol. 51, no. 9, pp. 3121–3145, September 2005.
- [20] A. Lozano, A. M. Tulino, and S. Verdù, "High-SNR power offset in multiantenna communication," *IEEE Transactions on Information Theory*, vol. 51, no. 12, pp. 4134–4151, December 2005.
- [21] F. Bøghagen, P. Orten, G. E. Øien, and S. de la Kethulle de Ryhove, "Exact capacity expressions for dual-branch Rician MIMO systems," *in press IEEE Transactions on Communications*, 2008.
- [22] I. Sarris and A. R. Nix, "Design and performance assessment of high-capacity MIMO architectures in the presence of a line-of-sight component," *IEEE Transactions on Vehicular Technology*, vol. 56, no. 4, pp. 2194–2202, July 2007.
- [23] M. Matthaiou, D. I. Laurenson, and C. -X. Wang, "Capacity study of vehicle-to-roadside MIMO channels with a line-of-

- sight component,” in *Proc. Wireless Communications and Networking Conference (WCNC)*, Las Vegas, USA, March 2008, pp. 775–779.
- [24] A. T. James, “Distributions of matrix variates and latent roots derived from normal samples,” *Annals of Mathematical Statistics*, vol. 35, no. 2, pp. 475–501, June 1964.
- [25] T. Ratnarajah, “Non-central quadratic forms on complex random matrices and applications,” in *Proc. Workshop on Statistical Signal Processing (SSP)*, Bordeaux, France, July 2005.
- [26] A. M. Mathai, *Jacobians of Matrix Transformations and Functions of Matrix Arguments*, Singapore: World Scientific, 1997.
- [27] C. G. Khatri, “On certain distribution problems based on positive definite quadratic functions in normal vectors,” *Annals of Mathematical Statistics*, vol. 37, no. 2, pp. 468–479, April 1966.
- [28] A. M. Sayeed, “Deconstructing multiantenna fading channels,” *IEEE Transactions on Signal Processing*, vol. 50, no. 10, pp. 2563–2579, October 2002.
- [29] K. Yu, M. Bengtsson, B. Ottersten, D. McNamara, P. Karlsson, and M. Beach, “Modeling of wideband MIMO radio channels based on NLoS indoor measurements,” *IEEE Transactions on Vehicular Technology*, vol. 53, no. 3, pp. 655–665, May 2004.
- [30] H. Boche and E. A. Jorswieck, “On the ergodic capacity as a function of the correlation properties in systems with multiple transmit antennas without CSI at the transmitter,” *IEEE Transactions on Communications*, vol. 52, no. 10, pp. 1654–1657, October 2004.
- [31] Ö. Oyman, R. Nabar, H. Bölcskei, and A. Paulraj, “Characterizing the statistical properties of mutual information in MIMO channels,” *IEEE Transactions on Signal Processing*, vol. 51, no. 11, pp. 2782–2795, November 2003.
- [32] M. Abramowitz and I. A. Stegun, *Handbook of Mathematical Functions With Formulas, Graphs, and Mathematical Tables*, New York: Dover, 1972.
- [33] “Draft amendment to wireless LAN medium access control (MAC) and physical layer (PHY) specifications: Wireless access in vehicular environments,” IEEE P802.11ptm/D2.01, March 2007.
- [34] A. P. Prudnikov, Y. A. Bruchkov, and O. I. Marichev, *Integrals and Series*, vol. 3, Gordon and Breach Science Publishers, 1990.

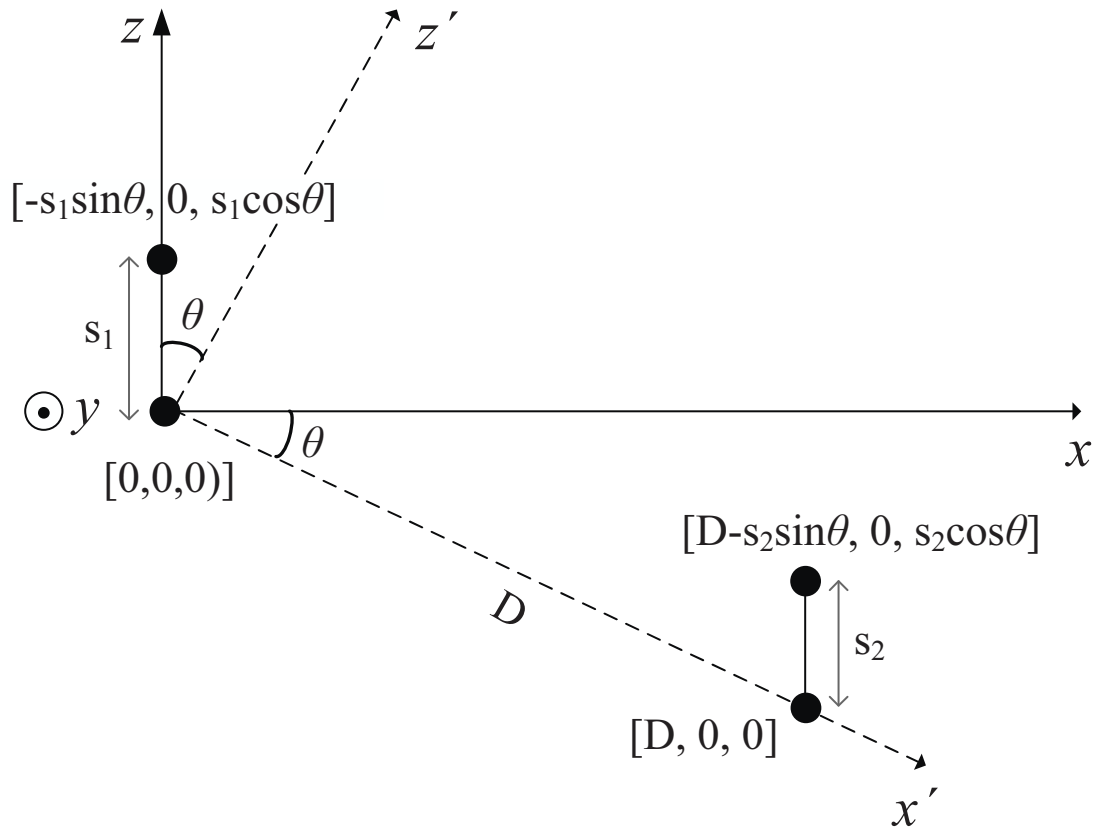
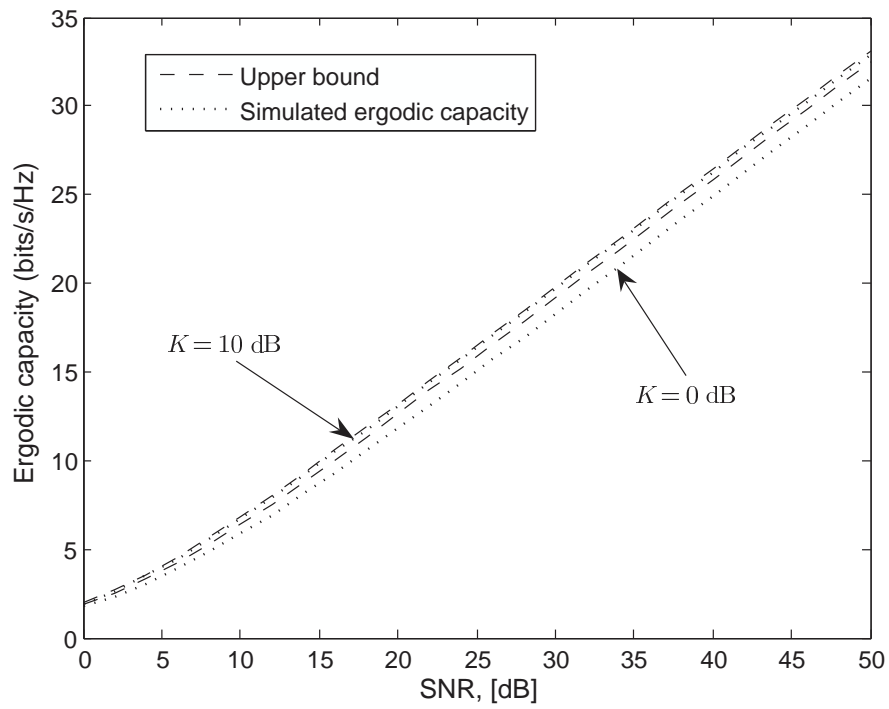
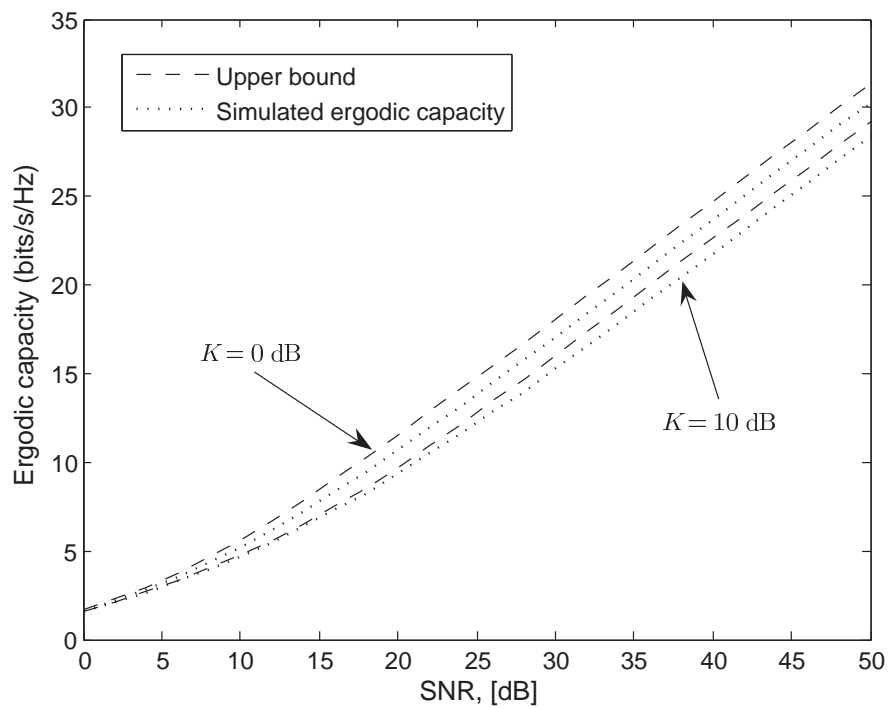


Fig. 1. A general architecture of a  $2 \times 2$  MIMO system with ULAs at both ends (side view). The coordinates of all elements with regard to the new coordinate system  $x'yz'$  are also included.



(a) Optimized configuration.



(b) Conventional configuration.

Fig. 2. Upper bound and ergodic capacity as a function of the SNR

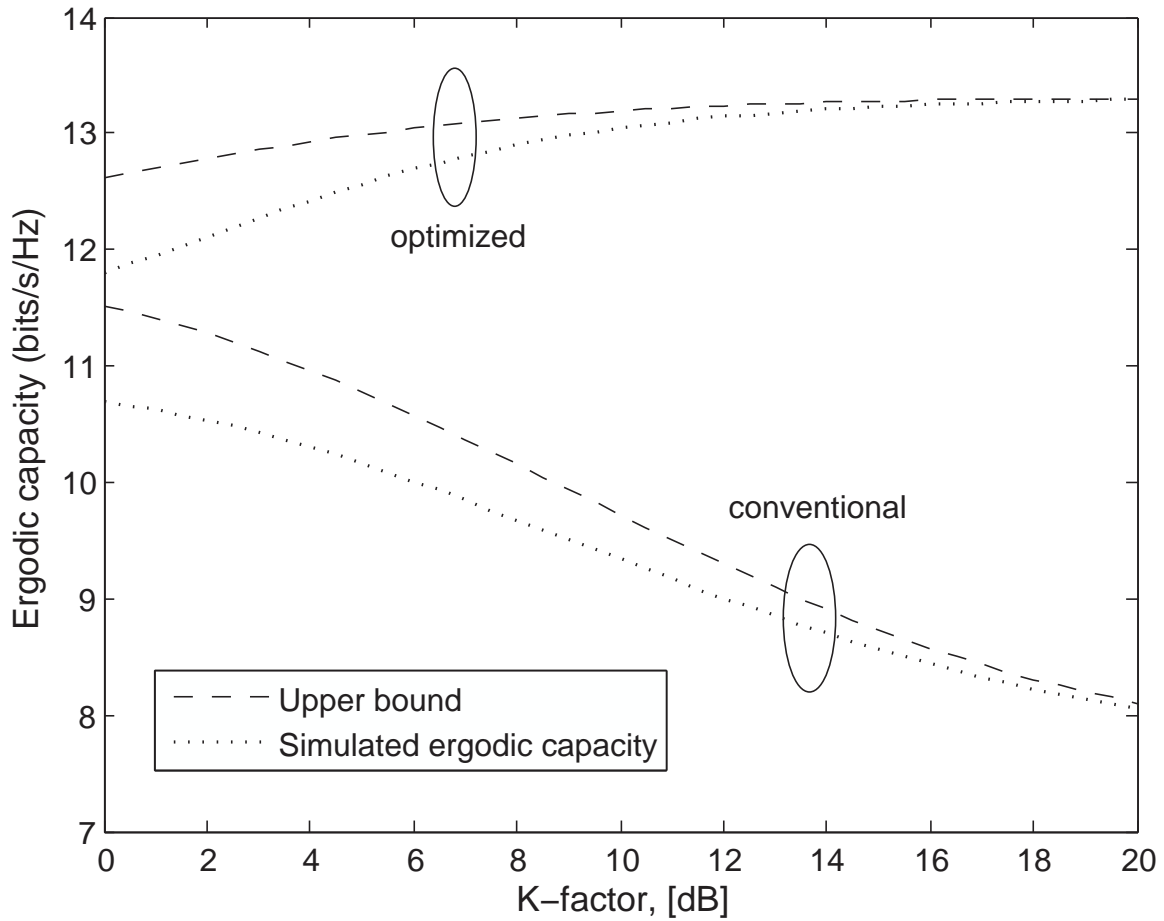


Fig. 3. Upper bound and ergodic capacity as a function of the  $K$ -factor ( $\delta_R = 0.2$ ,  $\delta_T = 0.5$  and  $\rho = 20$  dB).

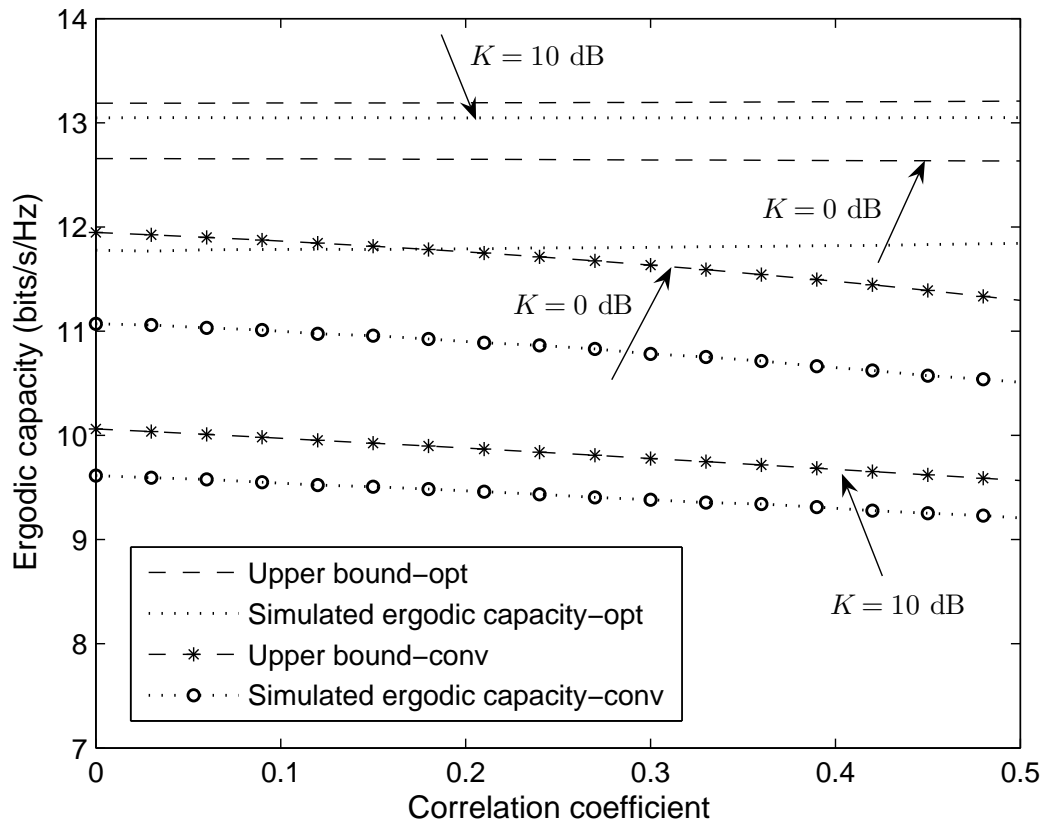


Fig. 4. Upper bound and ergodic capacity as a function of the correlation coefficients  $\delta_R$  and  $\delta_T$  ( $\rho = 20$  dB).

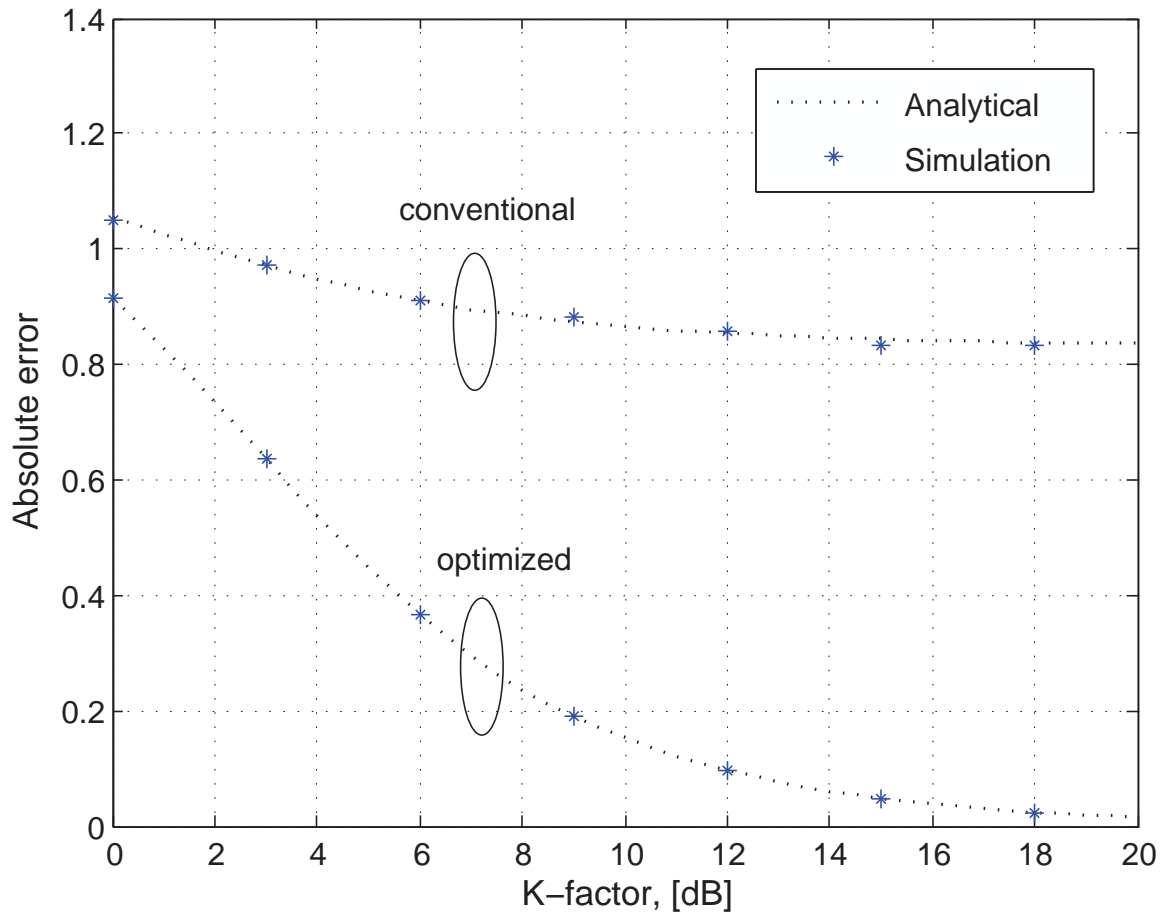


Fig. 5. Analytical and simulated absolute error of the upper bound in the high-SNR regime as a function of the  $K$ -factor ( $\delta_R = 0.2$  and  $\delta_T = 0.5$ ).